

# Presence of a central vein within white matter lesions on susceptibility weighted imaging: a specific finding for multiple sclerosis?

Nina Lummel · Tobias Boeckh-Behrens ·  
Veronika Schoepf · Michael Burke ·  
Hartmut Brückmann · Jennifer Linn

Received: 10 April 2010 / Accepted: 14 June 2010 / Published online: 29 June 2010  
© Springer-Verlag 2010

## Abstract

**Introduction** Susceptibility weighted imaging depicts the perivenous extent of multiple sclerosis white matter lesions (MS-WML) in vivo by directly visualizing their centrally running vein. The aim of this study was to investigate the specificity of this finding for MS.

**Methods** Fifteen patients with MS and 15 patients with microangiopathic white matter lesions (mWML) underwent 3T MRI, including a fluid-attenuated inversion recovery sequence (FLAIR) and a susceptibility weighted angiography (SWAN). All WMLs were identified on FLAIR and assigned to one of the following localizations: supratentorial peripheral, supratentorial periventricular, or infratentorial. Subsequently, the presence of a central vein within these lesions was assessed on SWAN.

**Results** A total of 711 MS-WMLs and 1,119 m-WMLs were identified on FLAIR, all of which could also be visualized on SWAN. A central vein was detectable in 80% of the MS-WMLs and in 78% of the m-WMLs (in 73% and 76% of the peripheral, in 92% and 94% of the periventricular, and in 71% and 75% of the infratentorial MS-WMLs and m-WMLs, respectively). With regard to the

supratentorial peripheral lesions, significantly more m-WMLs showed a central vein compared to the MS-WMLs. For the other localizations, there was no significant difference between the groups with regard to the percentage of lesions with central vein.

**Conclusions** Our results indicate that the detection of a central vein within a WML should not be considered a specific finding for MS; it is also found in WMLs of other etiologies.

**Keywords** Multiple sclerosis · Susceptibility weighted angiography · SWAN · MRI · FLAIR · Fluid-attenuated inversion recovery sequence

## Purpose

Multiple sclerosis (MS) is a chronic, multifocal, inflammatory disease of the central nervous system. The process of demyelination is reflected in white matter lesions (WMLs). Suggestive of MS can be juxtacortical lesions, irregular and confluent periventricular lesions, or lesions in the corpus callosum [1]. The morphology of lesions is also important; ovoid lesions and so-called Dawson's fingers are typically found in MS [2, 3]. Postmortem studies have shown that this typical distribution and form of MS lesions in the brain can be explained by their perivenous localization [2, 4].

WMLs on MRI are not a specific finding for MS, but are found in an abundance of other diseases. Hypertensive microangiopathy is one of the most common causes of WMLs, and microangiopathic WMLs (m-WMLs) are even found in a large percentage of clinically healthy elderly people [5–11]. Unlike in MS, m-WMLs are commonly located in the deep and subcortical white matter [12].

N. Lummel (✉) · T. Boeckh-Behrens · V. Schoepf ·  
H. Brückmann · J. Linn  
Department of Neuroradiology, University of Munich,  
Marchioninistrasse 15,  
81377 Munich, Germany  
e-mail: nina.lummel@med.uni-muenchen.de

V. Schoepf  
MR Centre of Excellence, Medical University of Vienna,  
Vienna, Austria

M. Burke  
GE Healthcare,  
Solingen, Germany

Arteriosclerosis due to arterial hypertension is thought to be the most important causative factor in the evolution of these lesions [13]. The pathohistological correlate of m-WMLs, areas of reduced myelination with atrophy of the neuropil around fibrohyalinotic arteries, as well as different stages of perivenous damage were found [14].

Concerning MRI, T2-weighted sequences such as long TR dual-echo, spin-echo or fluid-attenuated inversion recovery sequence (FLAIR) are well-established MRI techniques to detect WMLs. While FLAIR has the advantage of easily separating WMLs from CSF-like lesions, it tends to overestimate the number of lesions [15, 16] and might be less sensitive to the lesions in the posterior fossa [16]. Its reported sensitivity is 95% (87–99%) for periventricular WMLs and 86% (79–93%) for peripheral WMLs with a specificity of 71% (44–90%) and 80% (72–88%), respectively [17]. In order to enhance the diagnostic specificity in clinical routine, the identification of more specific morphologic characteristics of MS-WMLs would be helpful.

Recently, heavily T2-weighted MR techniques have been used to show the perivenous distribution of MS lesions—known from histopathological studies *in vivo* [18–20]. Different approaches can be used to acquire these so-called susceptibility weighted images (SWI) [18–23]. Susceptibility weighted angiography (SWAN), the method applied in this study, uses a 3D multi-echo gradient echo sequence in order to enhance the T2\* effect [22].

Hence, the aim of this study was to assess if a perivenous distribution of WMLs in MRI is a specific finding in MS patients.

## Methods

The study was approved by our institutional review board and informed consent was obtained from all patients who participated in the MR investigations.

### Subjects

In a prospective study, 15 patients with clinically definite MS (12 women, 3 men; mean age, 48.4 years; range, 21–70 years) were included. Twelve patients presented with a relapsing–remitting subtype of MS and three patients were diagnosed with secondary progressive MS. None of these patients had any evidence or prior diagnosis of cardiovascular morbidity, cerebrovascular disease, or other neurological disease.

In addition, we included 15 consecutive patients (7 women, 8 men; mean age, 69.2 years; range, 50–89 years) with WMLs, most probably due to hypertensive microangiopathy without any signs and symptoms of MS. All

patients with known stroke, manifest neurological deficit, and severe cortical atrophy were excluded.

### MRI acquisition

MR imaging was conducted on a 3.0 Tesla (T) system (Signa HDxt, GE Healthcare, Milwaukee, WI, USA) using an eight-channel head coil. The sequence protocol included a transversal FLAIR and a 3D SWAN sequence. For the FLAIR-weighted sequence, the image parameters were: repetition time (TR), 8,500 ms; echo time (TE), 120 ms; field of view (FOV), 200×200 mm; matrix, 320×320 mm; slice thickness, 5 mm, 23 slices; and acquisition time, 3 min 24 s. SWAN is a T2\*-weighted 3D-gradient echo pulse sequence, which acquires multiple echoes during one TR period at different timepoints [22]. The echoes are centered equidistantly in time on an effective TE in order to achieve a series of images with different TEs. From this series of images with different T2\* weightings, a collapsed image is calculated by building the sum of the squares of the different echoes. For this study an effective TE of 25.4 ms was chosen along with a receiver bandwidth of 62.5 kHz in order to achieve short echo spacing of 5.1 ms. Flip angle was chosen to be 20°; TR=43 ms; matrix size was 384×384 mm; FOV, 200×200 mm; slice thickness 2.6 mm; 60 slices; and acquisition time, 5 min 48 s.

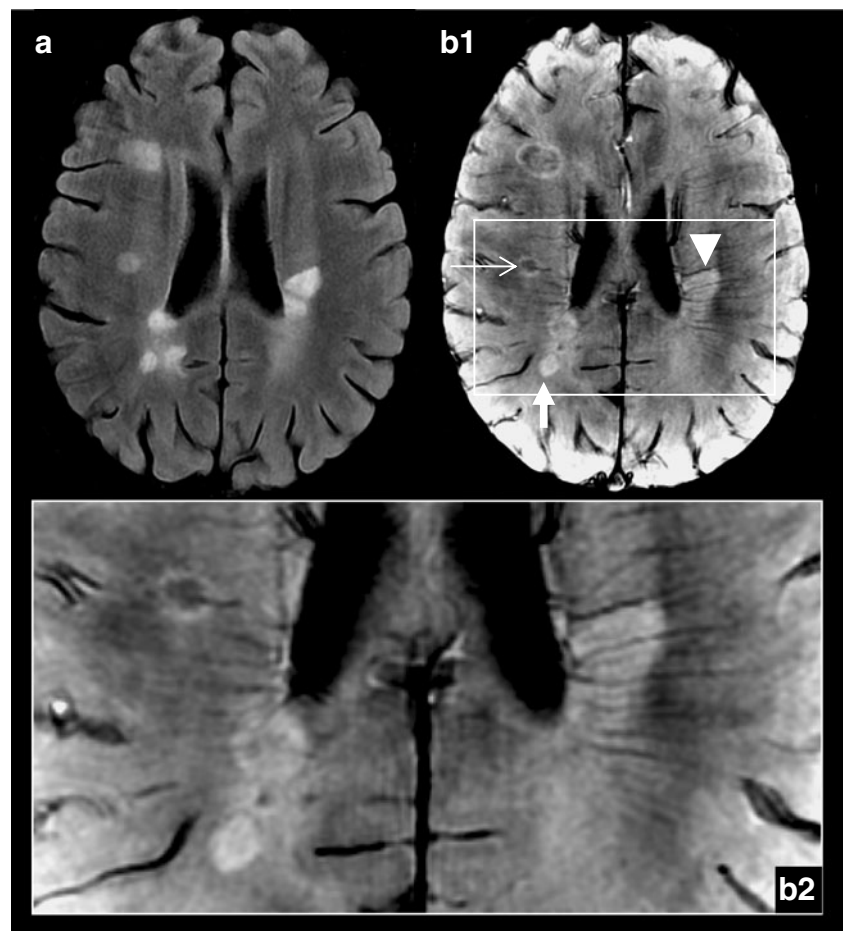
### Image analysis

The MR data sets were analyzed by two experienced neuroradiologists who were blinded to all clinical data and patient identification information. Blinding was performed by an instructed MR technician who made all the MR data sets anonymous by numbering them randomly. Image interpretation was performed on a standard picture archiving and communication system workstation.

FLAIR was used as gold standard for the identification of both MS-WMLs and m-WMLs. Each WML (size, >3 mm) was first identified on a FLAIR image and was classified as supratentorial periventricular, supratentorial peripheral, or infratentorial. Periventricular lesions were defined as those with a border within 4 mm of the ventricular surface [18]. All other supratentorial lesions were defined as peripheral.

In a second step, the correlate of each WML was identified on SWAN and it was assessed if a central vein, depicted as a hypointense structure running through the center of a respective lesion (Figs. 1 and 2), was identified on SWAN. Depending on the slice angle, the vein was either depicted as a thin dark line coursing through the center of the lesion (if it ran parallel to the acquisition plane) or as a small dark centrally located dot that could be tracked to adjacent slices (if the lesion, and thus the central

**Fig. 1** Axial FLAIR (**a**) and corresponding SWAN image (**b1**) of an MS-patient with magnified SWAN image in boxed area (**b2**). In most of the MS-WML, a central running vein can be identified as a linear hypointense structure running through the center of a respective lesion on SWAN (**b1**) *thin arrow*. Sometimes more than one vein can be identified within one lesion (**b1**) *arrowhead*. Furthermore, **b** shows an example of an MS-WML without a central vein that can be depicted (**b1**) *fat arrow*



vein, was orientated perpendicular to the imaging plane). Veins which did not run through the center of a lesion, but were located somewhere in its periphery, were not counted. Identification of the vein was based on the consensus between the two readers. Lesions were only classified as “lesion with a central vein” if both readers agreed on the identifiability of the centrally running vein. If the readers disagreed or were not sure about the presence of a central vein, the lesion was counted as being negative.

#### Statistics

For both patient groups (MS-WMLs and m-WMLs), the mean total lesion load was calculated. Ratios between the total number of plaques and the total number of veins in detected plaques were calculated for all patients of both groups. In addition, ratios were also calculated for peripheral, periventricular and infratentorial plaques in comparison to peripheral, periventricular and infratentorial plaques with veins, respectively. Frequencies were normally distributed (the test used for normal distribution was the Kolmogorov–Smirnov test). Mean ratios for all four variables (total number of plaques, peripheral, periventric-

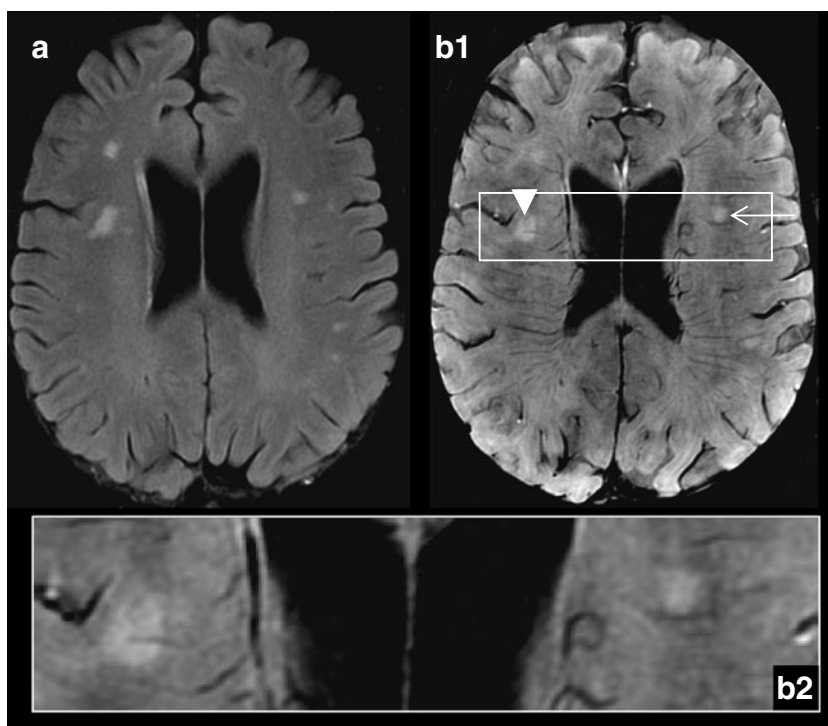
ular, and infratentorial plaques) between the two patient-groups were compared using a two-sample *t*-test. The data were analyzed using an SPSS (Version 17.0.2, SPSS Inc., Chicago, IL) statistical software, and a value of  $p < 0.05$  was considered significant.

#### Results

A total of 711 MS-WMLs and 1,119 m-WMLs were detected on FLAIR, all of which could also be identified on SWAN. In some lesions, especially in periventricular ones, more than one vein could be identified within a lesion (Fig. 1). In some patients, motion artifacts influenced the visibility of slightly small veins, but did not interfere with the analysis of the venograms.

In the MS patients, we found a lesion load of ten to 154 lesions per patient (mean,  $47 \pm 34$  lesions). Three hundred sixty one (50.8%) of the MS-WMLs were located at the supratentorial peripheral, 278 (39.1%) at the supratentorial periventricular, and 72 (10.1%) at the infratentorial. The frequency of m-WML ranged from 31 to 154 lesions per patient (mean,  $75 \pm 41$  lesions); 911, supratentorial periph-

**Fig. 2** Axial FLAIR (**a**) and corresponding SWAN image (**b1**) of a patient with m-WMLs with magnified SWAN image in boxed area (**b2**). The SWAN-sequence (**b**) shows one representative supratentorial peripheral lesion with a central vein (**b1**) arrowhead and one lesion where the vein passes next to the lesion, but does not cross it centrally (**b1**) arrow



eral (81.4%); 161, supratentorial periventricular (14.4%); and 47, infratentorial (4.2%) m-WMLs were found.

In total, a central vessel could be identified in 572 MS-WMLs (80.0%) and 875 m-WMLs (78.2%). In both groups periventricular lesions were more likely associated with a central vessel rather than a peripheral lesion (vessels seen in 91.7% (MS-WML) and 93.8% (m-WMLs), periventricular lesions; 73.1% (MS-WML) and 75.6% (m-WMLs), peripheral lesions) (for summary see Table 1).

For the periventricular and the infratentorial WMLs, there was no significant difference with regard to the ratio of “WMLs with central veins” versus the “total number of WMLs” between both groups. On the contrary, we found significantly more supratentorial peripheral lesions with central veins in the m-WML group compared to the MS-WML group ( $p=0.014$ ).

## Conclusions

In our study, central veins were equally present in both MS-WMLs and in m-WMLs. With regard to supratentorial peripheral lesions, central veins were even more often found in m-WMLs compared to MS-WMLs.

We used a multi-echo approach in order to get heavily T2\*-weighted images. The so-called susceptibility weighted (SW) sequences take advantage of the high susceptibility of materials with strong paramagnetic properties, for example, iron and venous blood. The high amount of deoxygenated hemoglobin leads to a relatively fast loss of

phase coherence of excited spins in venous compartments, and therefore, to a short T2\* relaxation time compared to the surrounding tissue. Thus, these heavily T2-weighted images are ideally suited to visualize venous vessels in great detail [24].

Due to the enhanced susceptibility effects of the ultra-high magnetic field scanners with field strengths of 7T or more, they provide heavily T2\*-weighted sequences even if a relatively short TE of 25 ms is used [20]. In 1.5T and 3T

**Table 1** Demographic patient data and lesion characteristics.

	MS-WML	m-WML
Number of patients	15	15
Sex (male/female)	3/12	8/7
Mean age (years)	48.4	69.2
Mean lesion load ( $\pm$ SD)	47 $\pm$ 34	75 $\pm$ 41
Total number of lesions		
On FLAIR	711	1,119
With central vein on SWAN (no./%)	572/80.0	875/78.2
Peripheral lesions		
On FLAIR	361	911
With central vein on SWAN (no./%)	264/73.1	689/75.6
Periventricular lesions		
On FLAIR	278	161
With central vein on SWAN (no./%)	255/91.7	151/93.8
Infratentorial lesions		
On FLAIR	72	47
With central vein on SWAN (no./%)	51/70.8	35/74.5



scanners, however, a long TE is needed to get a strong T2\* effect. Single-echo-long TE scans lead to the problem of geometric distortion and chemical shift artifacts. The SWI method or, so-called, MR venography does overcome this drawback by masking the long TE magnitude-contrast images with the corresponding phase-contrast images. In SWAN, another approach is used to reduce the artifacts due to the long TE [22]. Here, a series of magnitude images with different TEs is acquired in order to calculate a weighted sum of these multiple echoes. Since the multiple echoes are collected within one TR acquisition, it is not prolonged compared to the duration needed to acquire a single echo. The results are heavily SWIs, which are visually comparable to those generated using the SWI technique introduced by Reichenbach et al. [24] (Fig. 3). Nevertheless, a systematic comparison of the SWAN versus the SWI sequence has not yet been performed to our knowledge. As a potential benefit of the SWAN approach, the averaging of several images results in a higher signal to noise ratio. A disadvantage of the SWAN technique compared to the SWI might be that the phase information is not available.

Mainly due to the phase information, veins are best visualized in the transverse orientation in the SWI sequence [25]. It has not been evaluated yet if the orientation of the acquisition has an impact on the visualization of the veins in the SWAN sequence as well, although the phase information is not taken into account in this sequence. Nevertheless, we chose the transverse plane for the SWAN sequence in this investigation.

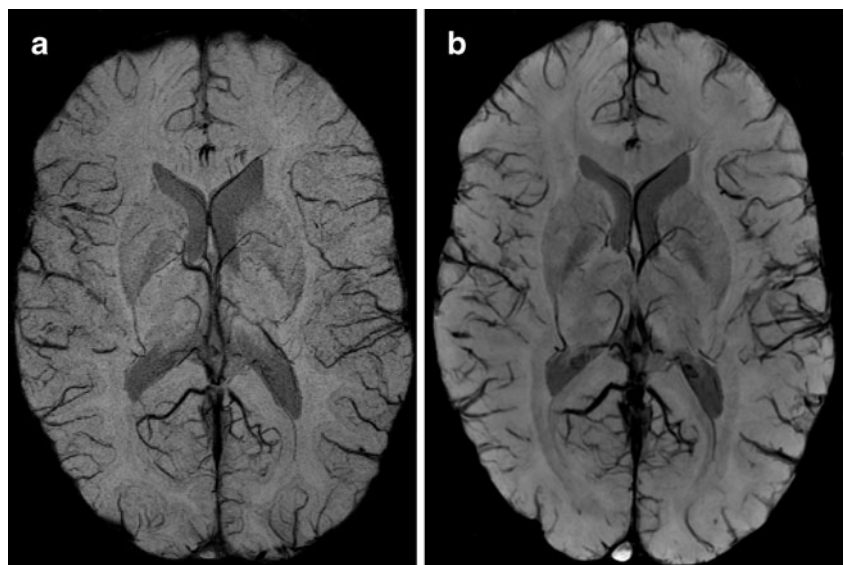
With regard to MS, heavily T2\*-weighted images have been used to characterize MS-WMLs in more detail [26]. At 7T, a multilayer structure of regions with different signal intensities and a hypointense rim in larger plaques (>10 mm) could be depicted. In addition, SW imaging

accomplished the *in vivo* imaging of the perivenous distribution of MS-WMLs, which was only known before from histopathologic studies [2, 27, 28]. While all studies consistently found central veins within MS plaques, the percentage of plaques with central veins varied depending on the field strength and sequence used on the one hand and the localization of the plaques on the other hand. In consensus with our findings, periventricular MS-WMLs showed a central vein in a higher percentage (96 to 100%) compared to peripheral plaques (65%) [18, 19, 29]. As a possible explanation, it has been hypothesized that the pathogenic mechanisms underlying lesion formation differ depending on the localization of the MS-WMLs [28]. In addition, it is possible that peripheral lesions, which tend to be smaller than periventricular lesions, are more likely to contain blood vessels which are beyond our spatial resolution. This is supported by the fact that high-resolution 7T MRI detected associated vessel in all MS lesions—even in those smaller than 3 mm [29]. In order to minimize this fault, we included only lesions with a diameter of more than 3 mm.

Furthermore, the fact that a central vein could also be delineated less often in infratentorial-located lesions could be explained in an analogous manner. Tan et al. [19] demonstrated that MS lesions as well as (small) veins could not be confidently identified in the parenchyma near the air-tissue interfaces around the sinuses or in the mastoid and infratentorial regions using SWI. In SW images iron-containing structures, such as the red nucleus, the substantia nigra and the globus pallidus, also adjacent air within bony structures of the skull base produce marked signal loss and artifacts, respectively [19].

It has been suggested that the identification of a central vein within a WML might be a specific finding for MS.

**Fig. 3** Corresponding axial SWI (a) and SWAN (b) of a healthy volunteer. The images were obtained on two different 3T MRI scanners (a Signa HDxt, GE Healthcare, Milwaukee, WI, USA; b Magnetom Verio, Siemens Healthcare, Erlangen, Germany)



Yet, we did not only find a central vein in the majority of MS lesions (80%), but also in the majority of m-WMLs (78%). Analog to MS-WMLs, the veins within the m-WMLs were located in the center of the lesion. With regard to all lesions as well as with regard to both periventricular and infratentorial lesions alone, there were no significant differences concerning the percentage of MS-WMLs with central veins versus m-WMLs with central veins. For peripheral WMLs, the percentage of m-WMLs with central veins was even higher than that of the MS-WMLs. In both patient groups, periventricular lesions showed a central vein more often than peripheral ones.

In addition to central veins, we incidentally observed single or multiple veins at the periphery of both MS-WMLs and m-WMLs (as shown in Fig. 1). Yet, in agreement with histopathologic studies and previous MR studies [2, 19], we focused on centrally running veins and disregarded peripheral veins.

As veins and venules are ubiquitous, there is a certain chance that they traverse any type of WML coincidentally. Tan et al. [19] discuss the presence of veins within hypoxic ischemic WMLs as an incidental finding on SWI, but did not investigate this issue systematically. They hypothesize that the mere presence of a small vein within a lesion might not be more than coincidence, while the correspondence of ovoid lesions along a vein was typical for MS [19]. However, patients showing only the classical morphological findings for MS with typically ovoid predominantly periventricular lesions do not represent a great diagnostic challenge for the radiologist. Yet, patients in whom, at least part of the lesions are unequivocal in shape and localization, are the ones whose additional MS-specific findings would be very helpful. Thus, we did not take into account the shape of the individual lesion in our analysis, but focused purely on the presence of a central vein. Our results do not support the hypothesis that the presence of a central vein on SW imaging is a specific finding for MS [18–20].

In addition to the above-mentioned applications of SW imaging in MS, the technique has also been reported to be superior to FLAIR with regard to the number of identified MS lesions [30]. We used FLAIR as the gold standard for WMLs because it is especially sensitive to white matter pathologies [31, 32]. Thus, our results cannot give information about the potential superiority of SWAN compared to the FLAIR in detecting WMLs. A comparison of these two sequences regarding the sensitivity in detecting WMLs is limited anyway, since they are measuring different features, one T2 weighting and the other the susceptibility phase. Previous studies have shown that the two methods are complementary in that SWI sees some lesions not seen by T2 imaging and vice versa [30, 33]. Nevertheless, in this study all WMLs (MS and micro-

angiopathic) detected on FLAIR were also reliably visualized on SWAN.

As a limitation to this study the problem of the quantification of WMLs has to be mentioned. In this study, two neuroradiologists counted the WMLs in consensus and did not use semi- or fully-automated quantification methods. Furthermore, we did not account for the size of the lesions. Hence, a correlation between the size of the lesion and the presence of a central vein could not be performed. Another limitation is the consideration of the infratentorial lesions as both sequences, FLAIR and SW imaging, have their limitations in the infratentorial region. Furthermore, the slice thickness between the FLAIR (5 mm) and the SWAN (2.6 mm) sequence has to be mentioned. Since we did not aim to compare the sensitivity of the SWAN and the FLAIR regarding the detection of WMLs, but to access the differential diagnostic value of the depiction of a central vein within a certain WML, the aforementioned limitations do not necessarily influence our conclusions.

In summary, the results of this study indicate that the detection of a central vein within a WML cannot be considered a specific finding for MS. As far as MR imaging is concerned, the typical distribution and shape of the lesions are up to the present still the major criteria for the diagnosis of MS.

**Conflict of interest statement** We declare that we have no conflict of interest.

## References

1. Victor M, Ropper AH (2005) Adams and Victor's Principles of Neurology. McGraw-Hill, New York
2. Fog T (1965) The topography of plaques in multiple sclerosis with special reference to cerebral plaques. *Acta Neurol Scand Suppl* 15:1–161
3. Horowitz AL, Kaplan RD, Grewe G, White RT, Salberg LM (1989) The ovoid lesion: a new MR observation in patients with multiple sclerosis. *AJNR Am J Neuroradiol* 10:303–305
4. Putnam TJ (1933) The pathogenesis of multiple sclerosis: a possible vascular factor. *N Engl J Med* 209:786–790
5. Ylikoski A, Erkinjuntti T, Raininko R, Sarna S, Sulkava R, Tilvis R (1995) White matter hyperintensities on MRI in the neurologically nondiseased elderly. Analysis of cohorts of consecutive subjects aged 55 to 85 years living at home. *Stroke* 26:1171–1177
6. Pantoni L, Garcia JH (1995) The significance of cerebral white matter abnormalities 100 years after Binswanger's report. A review. *Stroke* 26:1293–1301
7. Breteler MM, van Swieten JC, Bots ML, Grobbee DE, Claus JJ, van den Hout JH, van Harskamp F, Tanghe HL, de Jong PT, van Gijn J et al (1994) Cerebral white matter lesions, vascular risk factors, and cognitive function in a population-based study: the Rotterdam Study. *Neurology* 44:1246–1252
8. de Leeuw FE, de Groot JC, Achten E, Oudkerk M, Ramos LM, Heijboer R, Hofman A, Jolles J, van Gijn J, Breteler MM (2001)

- Prevalence of cerebral white matter lesions in elderly people: a population based magnetic resonance imaging study. The Rotterdam Scan Study. *J Neurol Neurosurg Psychiatry* 70:9–14
9. Hopkins RO, Beck CJ, Burnett DL, Weaver LK, Victoroff J, Bigler ED (2006) Prevalence of white matter hyperintensities in a young healthy population. *J Neuroimaging* 16:243–251
  10. Launer LJ, Berger K, Breteler MM, Dufouil C, Fuhrer R, Giampaoli S, Nilsson LG, Pajak A, de Ridder M, van Dijk EJ et al (2006) Regional variability in the prevalence of cerebral white matter lesions: an MRI study in 9 European countries (CASCADE). *Neuroepidemiology* 26:23–29
  11. Wen W, Sachdev P (2004) The topography of white matter hyperintensities on brain MRI in healthy 60- to 64-year-old individuals. *Neuroimage* 22:144–154
  12. Uhlenbrock D, Sehlen S (1989) The value of T1-weighted images in the differentiation between MS, white matter lesions, and subcortical arteriosclerotic encephalopathy (SAE). *Neuroradiology* 31:203–212
  13. van Swieten JC, van den Hout JH, van Ketel BA, Hijdra A, Wokke JH, van Gijn J (1991) Periventricular lesions in the white matter on magnetic resonance imaging in the elderly. A morphometric correlation with arteriolosclerosis and dilated perivascular spaces. *Brain* 114(Pt 2):761–774
  14. Fazekas F, Kleinert R, Offenbacher H, Payer F, Schmidt R, Kleinert G, Radner H, Lechner H (1991) The morphologic correlate of incidental punctate white matter hyperintensities on MR images. *AJNR Am J Neuroradiol* 12:915–921
  15. Bakshi R, Caruthers SD, Janardhan V, Wasay M (2000) Intraventricular CSF pulsation artifact on fast fluid-attenuated inversion-recovery MR images: analysis of 100 consecutive normal studies. *AJNR Am J Neuroradiol* 21:503–508
  16. Tanaka N, Abe T, Kojima K, Nishimura H, Hayabuchi N (2000) Applicability and advantages of flow artifact-insensitive fluid-attenuated inversion-recovery MR sequences for imaging the posterior fossa. *AJNR Am J Neuroradiol* 21:1095–1098
  17. Fernando MS, O'Brien JT, Perry RH, English P, Forster G, McMeekin W, Slade JY, Golkhar A, Matthews FE, Barber R et al (2004) Comparison of the pathology of cerebral white matter with post-mortem magnetic resonance imaging (MRI) in the elderly brain. *Neuropathol Appl Neurobiol* 30:385–395
  18. Tallantyre EC, Brookes MJ, Dixon JE, Morgan PS, Evangelou N, Morris PG (2008) Demonstrating the perivascular distribution of MS lesions in vivo with 7-Tesla MRI. *Neurology* 70:2076–2078
  19. Tan IL, van Schijndel RA, Pouwels PJ, van Walderveen MA, Reichenbach JR, Manoliu RA, Barkhof F (2000) MR venography of multiple sclerosis. *AJNR Am J Neuroradiol* 21:1039–1042
  20. Ge Y, Zohrabian VM, Osa EO, Xu J, Jaggi H, Herbert J, Haacke EM, Grossman RI (2009) Diminished visibility of cerebral venous vasculature in multiple sclerosis by susceptibility-weighted imaging at 3.0 Tesla. *J Magn Reson Imaging* 29:1190–1194
  21. Haacke EM, Xu Y, Cheng YC, Reichenbach JR (2004) Susceptibility weighted imaging (SWI). *Magn Reson Med* 52:612–618
  22. Annamraju RB, Venkatesan R, Vu AT (2008) T2\* weighted angiography (SWAN): T2\* weighted non-contrast imaging with multi-echo acquisition and reconstruction. *ESMRMB abstract* 482
  23. Linn J, Bruckmann H (2010) Cerebral venous and dural sinus thrombosis: state-of-the-art imaging. *Klin Neuroradiol*. doi:10.1007/s00062-010-9035-7
  24. Reichenbach JR, Venkatesan R, Schillinger DJ, Kido DK, Haacke EM (1997) Small vessels in the human brain: MR venography with deoxyhemoglobin as an intrinsic contrast agent. *Radiology* 204:272–277
  25. Haacke EM, Mittal S, Wu Z, Neelavalli J, Cheng YC (2009) Susceptibility-weighted imaging: technical aspects and clinical applications, part 1. *AJNR Am J Neuroradiol* 30:19–30
  26. Wattjes MP, Barkhof F (2009) High field MRI in the diagnosis of multiple sclerosis: high field-high yield? *Neuroradiology* 51:279–292
  27. Adams CW, Poston RN, Buk SJ (1989) Pathology, histochemistry and immunocytochemistry of lesions in acute multiple sclerosis. *J Neurol Sci* 92:291–306
  28. Lassmann H, Wekerle H (2005) The pathology of multiple sclerosis. In: Compston A (ed) *McAlpine's multiple sclerosis*. Elsevier, London, pp 557–599
  29. Kollia K, Maderwald S, Putzki N, Schlamann M, Theysohn JM, Kraff O, Ladd ME, Forsting M, Wanke I (2009) First clinical study on ultra-high-field MR imaging in patients with multiple sclerosis: comparison of 1.5T and 7T. *AJNR Am J Neuroradiol* 30:699–702
  30. Haacke EM, Makki M, Ge Y, Maheshwari M, Sehgal V, Hu J, Selvan M, Wu Z, Latif Z, Xuan Y, Khan O, Garbern J, Grossman RI (2009) Characterizing iron deposition in multiple sclerosis lesions using susceptibility weighted imaging. *J Magn Reson Imaging* 29:537–544
  31. Bastianello S, Bozzao A, Paolillo A, Giugni E, Gasperini C, Koudriavtseva T, Millefiorini E, Horsfield MA, Colonnese C, Toni D et al (1997) Fast spin-echo and fast fluid-attenuated inversion-recovery versus conventional spin-echo sequences for MR quantification of multiple sclerosis lesions. *AJNR Am J Neuroradiol* 18:699–704
  32. Rovaris M, Rocca MA, Yousry I, Yousry TA, Colombo B, Comi G, Filippi M (1999) Lesion load quantification on fast-FLAIR, rapid acquisition relaxation-enhanced, and gradient spin echo brain MRI scans from multiple sclerosis patients. *Magn Reson Imaging* 17:1105–1110
  33. Eissa A, Lebel RM, Korzan JR, Zavodni AE, Warren KG, Catz I, Emery DJ, Wilman AH (2009) Detecting lesions in multiple sclerosis at 4.7 tesla using phase susceptibility-weighting and T2-weighting. *J Magn Reson Imaging* 30:737–742